Generalized Parton Distribution studies with CLAS at JLab

Brahim Moreno[1] *

Université Paris-Sud 11, Institut de Physique Nucléaire d'Orsay
15 rue Georges CLEMENCEAU 91406 ORSAY - France

Generalized Parton Distributions (GPDs) [2] parameterize the non-perturbative structure of the nucleon and can be used to reveal the correlations between the momentum and position of partons in the nucleon. They appear in the amplitudes of hard-exclusive electroproduction reactions such as DVCS on the nucleon, $ep \to e'p'\gamma$, and Deeply Virtual Meson Production (DVMP). Among all the experimental GPD studies that were carried out using data collected with the CLAS detector [3], recent results will be presented. This includes the Beam Spin Asymmetry (BSA) for DVCS and π^0 leptoproduction as well as the cross section for ρ^0 electroproduction.

1 Generalized Parton Distributions and deeply virtual scattering processes

The introduction of Generalized Parton Distributions in the 1990's [2] renewed the study of the nucleon structure. These functions can be seen as a generalization of both form factors (FFs) and parton distribution functions (PDFs). Indeed, they give the correlation between space and momentum information of partons in the nucleon. GPDs depend on three kinematical variables: ξ, x and t, the latter being the square of the momentum transfered to the nucleon. The variables ξ and x reflect the longitudinal momentum fraction transfered to the probed quark and the longitudinal momentum fraction of the probed quark, respectively (see Fig. 1 for their illustration). The simplest process used to access these functions is Deeply Virtual Compton Scattering (DVCS) which is described hereafter.

1.1 DVCS

The DVCS process involves, in our case, the scattering of an electron off the proton with the production in the final state of a hard photon ($ep \to e'p'\gamma$). At small t and in the Bjorken limit, the DVCS amplitude factorizes into two parts: a *hard* part, exactly calculable and purely electromagnetic and a *soft* part describing the non-perturbative structure of the nucleon (see Fig. 1, left hand side). The Bjorken limit is defined as: large $Q^2 = -(k - k')^2$ and fixed $x_{Bj} = Q^2/2(p \cdot q)$, with k, k', p, q, the four-vectors of the incoming and outgoing electron, the proton target and the virtual photon respectively. DVCS is one of the two main processes that contribute to the $ep \to e'p'\gamma$ reaction in the limit described above. The other one is the Bethe-Heitler process, where the produced photon is emitted by the incoming or the outgoing electron. The two processes interfere and when using a polarized lepton beam this produces an asymmetry between positive and negative beam helicity states. This Beam Spin Asymmetry can be parameterized as a function of ϕ [4], the angle between the leptonic plane (defined by the incoming and the outgoing electron) and the hadronic plane

*For the CLAS collaboration.

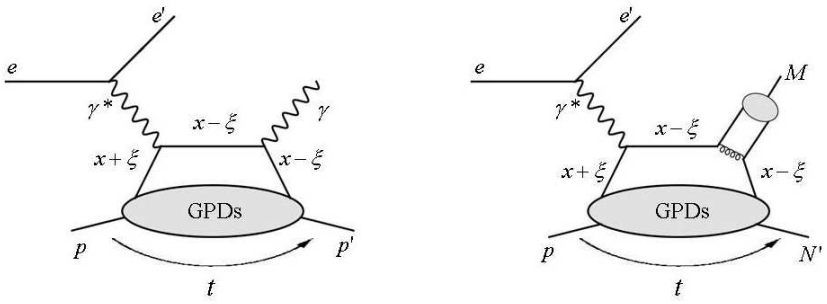

Figure 1: Deeply virtual scattering process diagrams. On the left-hand side: the DVCS *handbag* diagram. On the right-hand side: the DVMP *handbag* diagram.

(defined by the produced photon and the recoil hadron): $A \simeq \alpha sin\phi/(1+\beta cos\phi)$ (twist-2 approximation). The parameters α and β are related to integrals of GPDs. Therefore, measuring the beam spin asymmetry for the DVCS process is a way of accessing GPDs.

1.2 DVMP

Of great interest is also the exclusive DVMP $ep \to e'N'M$ where N' is the recoil nucleon and M the meson produced (for associated diagram see Fig. 1, right hand side). As in the DVCS case the electroproduction of mesons $ep \to e'N'M$ can be factorized in the high Q^2 and low t limit. The factorization, in this case, has only been proven for longitudinally polarized virtual photons. One of the motivations for studying DVMP is that, depending on the meson produced, the process is sensitive to different quark-flavoured GPD combinations allowing flavour decomposition of these functions. Moreover there is a difference between vector and pseudoscalar mesons. The production of vector mesons involves helicity independent GPDs while pseudoscalar mesons production involves helicity dependent ones. Indeed, DVMP is a very interesting tool to extract GPDs but the involvement of quark-gluon coupling and of distribution amplitudes makes it less straightforward to treat than DVCS when it comes to data interpretation.

2 Experimental studies of deeply virtual scattering processes with CLAS

2.1 Photon electroproduction $ep \to e'p'\gamma$

2.2 Event selection

Due to the missing mass resolution of the CLAS detector which does not allow the separation between a π^0 and a photon, the detection of all final state particles is required. The selection is done through cuts applied to several quantities, such as the missing mass squared of the $ep \to e'p'\gamma X$ system. There is still some remaining background after applying cuts. It comes from partially measured π^0 electroproduction where only one of the two decay photons is detected. This background is estimated and subtracted using Monte-Carlo simulations and

exclusive π^0 electroproduction data. The amount varies with kinematics and is 5% on average. For more details on the analysis see [5].

2.3 Results

The DVCS beam spin asymmetry has been measured over a wide kinematical range. The asymmetries were fitted with the following function: $A = \alpha sin\phi/(1+\beta cos\phi)$. The extracted α parameter (the asymmetry at $\phi = 90^o$) is shown in Fig. 2 (full circles) for each (Q^2, x_B) bin, as a function of t. The comparison between data and the calculations based on the

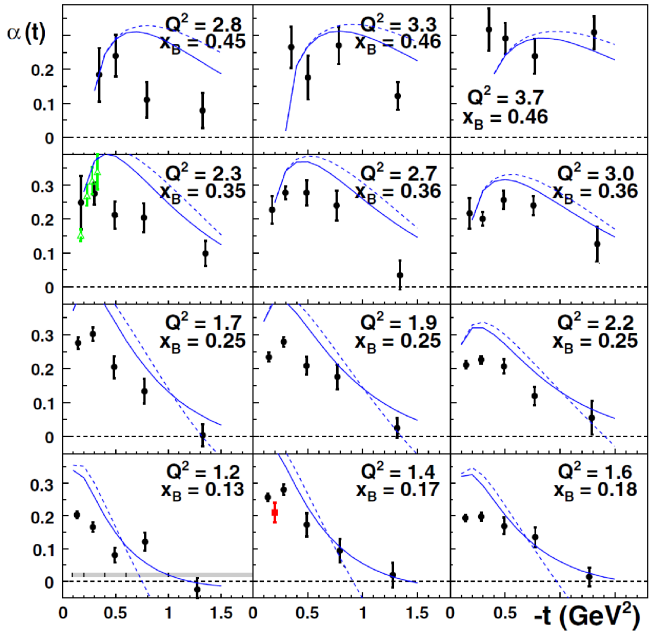

Figure 2: Extracted α parameter for the DVCS Beam Spin Asymmetry. The full square corresponds to a previous CLAS result [6] while open triangles correspond to previous Hall A data [7]. The grey band in the lower left hand side plot illustrates the size of the systematic uncertainties. The solid and dashed curves are GPD parameterizations using the VGG code with twist-2 [8] and twist-3 [9] approximations respectively.

GPD parameterizations of the VGG code [8, 9] shows a qualitative agreement: the decrease of α is reasonably well reproduced at large $-t$ as well as the behaviour at small $-t$ for the highest Q^2 bins i.e. the latter being the region where the factorization is supposed to be valid (small $-t$, large Q^2). However, the parameterization exceeds the data at small $-t$ in almost all other kinematics.

2.4 π^0 electroproduction $ep \to e'p'\pi^0 \to e'p'\gamma\gamma$

2.5 Event selection

The identification procedure of exclusive π^0 leptoproduction events is almost the same as in the DVCS case. First it is required that all final state particles be detected. Then, selection cuts are applied to several quantities such as missing masses. A sideband subtraction method (a detailed example of which can be found in [10]) was used for this analysis as a complementary tool to identify the π^0 and $e'p'\pi^0$ events. The detailed analysis can be found in [11].

2.6 Results

The beam spin asymmetry for the $ep \to' ep'\pi^0$ channel has been measured over the same kinematical range as the DVCS analysis described previously. The asymmetries were fitted with the following function: $A = \alpha sin\phi$. The extracted α parameter is shown in figure 3 for each kinematical bin as a function of t. It is clearly different from zero within the error bars. The asymmetries are of the order of 4 to 11 %. This is a clear sign for an L/T interference which in turn might be the sign that the scaling regime is not yet reached. As a consequence if one wants to push this study further one has to perform a cross section measurement in order to perform an L/T separation and subsequently extract the longitudinal part of the cross section for comparison with GPD-based calculations.

2.7 ρ^0 electroproduction $ep \to e'p'\rho^0 \to e'p'\pi^+(\pi^-)$

2.8 Event selection

In this case, not all the final state particles were detected. The π^- originating from the decay of the ρ^0 was identified by the missing mass technique. The ρ^0 yield was then extracted by fitting the normalized distributions of the missing mass squared of the $ep \to e'p'X$ system for each elementary bin. As expected, for $e'p'\rho^0$ events a peak at the ρ^0 mass is visible in this distribution. For further details on the analysis see [12].

2.9 Results

The longitudinal cross section was extracted, based on SCHC (S-Channel Helicity Conservation) and on the analysis of pions angular decay distributions in the rho center of mass frame, for comparison with GPD model predictions. In Fig. 4, the total longitudinal cross section, as obtained from the analysis sketched previously, is plotted as a function of $W = \sqrt{(q+p)^2}$ along with the current world data. In the region of overlap, CLAS results are compatible with those of other experiments. Looking at the trend of the cross section, one clearly sees two regions: at low W the cross section decreases rapidly (almost one order of magnitude in some bins). It then flattens at intermediate W ($W \simeq 5$ GeV) and begins to rise slowly. The GPD calculations (dashed and thin solid curve) reproduce the data quite well in the intermediate and high W region. However they completely miss the data at small W. It is possible that in this region the factorization is not valid and so the data are not interpretable in terms of the handbag diagram. Also a contribution could be missing in the GPD parameterization in this region. The addition in the VGG model of a term whose amplitude is fitted to the data makes it possible to reproduce the data trend in the small W region.

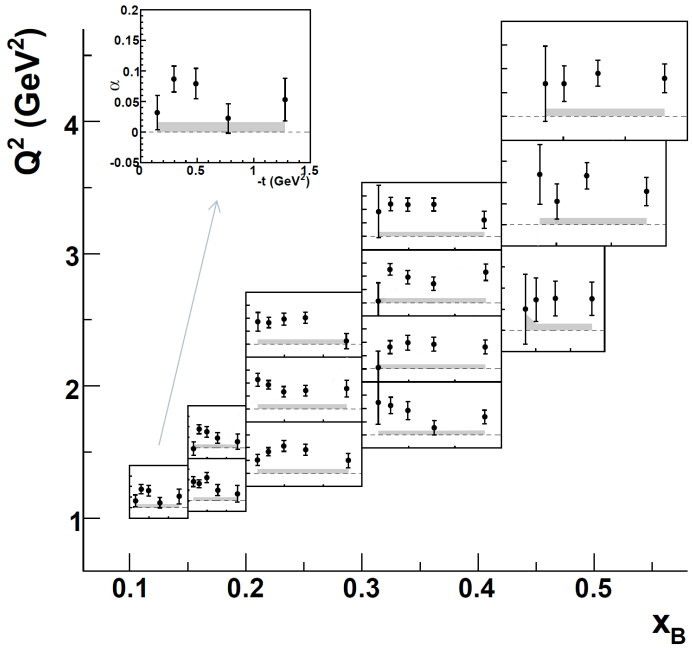

Figure 3: Extracted α parameter for $ep \to e'p'\pi^0$ Beam Spin Asymmetry. The upper left hand side plot is an enlargement of the lower left hand side one. It shows the axes, common to all plots. The shaded area shows the maximal size of the systematic uncertainties.

This term is used to amplify the contribution from the region between $x = \xi$ and $x = -\xi$ which increases as W decreases. However, the application of this term for comparison with experimental data is not yet fully understood. This is work in progress.

3 Conclusion

Recent CLAS DVCS Beam Spin Asymmetry results which cover the widest phase space in the valence region for such a channel were presented. It appears that data are consistent with previous measurements in overlapping regions. The region at high Q^2 and small t, where the handbag picture is thought to be valid, is reasonably well reproduced by GPD calculations, but not for all kinematics. The non-zero amplitude of the BSA for π^0 electroproduction is interpreted as a clear sign of an L/T interference. It means that if one wants to push this study further one has to perform a cross section measurement in order to extract the longitudinal part of the cross section for comparison with GPD-based calculations. CLAS data obtained for ρ^0 electroproduction show a good agreement with world data. They can be reproduced with the introduction of a term, whose amplitude is fitted to the data, in the VGG code . More work is needed to fully understand this.

There is more to come in the future. For instance, an exploratory study for ΔVCS BSA,

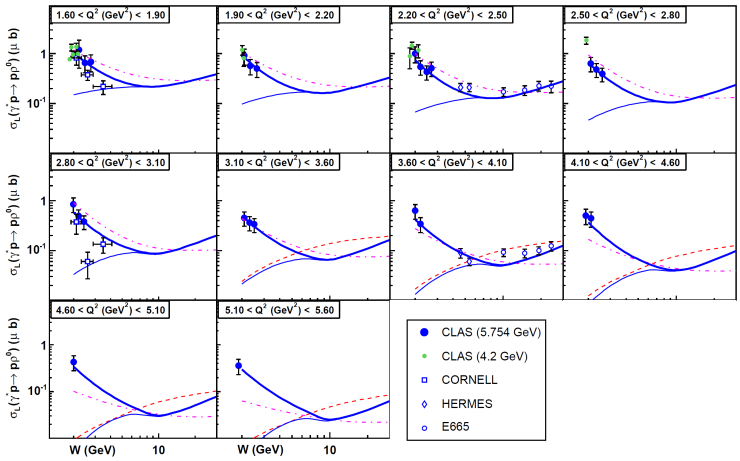

Figure 4: World data for the reduced cross section $\gamma^* p \to p' \rho^0_L$ as a function of W. The dashed and the thin solid curves show the results of the GK [13] and VGG calculations, respectively. The thick solid curve is the result of the VGG calculation with the addition of an extra contribution in the GPD parameterization which was fitted to the data [14]. The dot-dashed curve shows the results of a Regge-model calculation [15]. The 4.2 GeV CLAS, CORNELL, HERMES and E665 data are from references [16, 17, 18, 19], respectively.

the production of a Δ^+ resonance and a hard photon off the nucleon, is underway [20]. The final goal of the study is to better understand the nucleon to Δ transition with the use of transition GPDs which give a description of this transition at the partonic level. Also, the cross section for ρ^+ electroproduction is under study [21]. This work, as well as the measurement of the BSA for η leptoproduction, is part of the CLAS collaboration DVMP effort. There is also an ongoing effort to extract cross sections for DVCS and π^0 electroproduction from CLAS data. At a longer time scale, the upgrade of the CLAS detector [22] will be an essential tool for the study of deeply virtual scattering processes with a sizeable increase in the accessible phase space.

References

[1] Slides:
`http://indico.cern.ch/contributionDisplay.py?contribId=187&sessionId=25&confId=53294`

[2] D. Müller, D. Robaschik, B. Geyer, F.-M. Dittes, J. Hořejši, Fortsch. Phys. Nucl. Phys. **42** 101 (1994);
X. Ji, Phys. Rev. **D55** 7114 (1997);
A.V. Radyushkin, Phys. Rev. **D56** 5524 (1997).

[3] B.A. Mecking *et al.*, Nucl. Instrum. Meth. **A503** 513 (2003).

[4] A.V. Belitsky, D. Mueller and A. Kirchner, Nucl. Phys. **B629** 323 (2002).

[5] F.-X. Girod, Thèse de doctorat, Université Louis Pasteur (Strasbourg) (2006);
F.-X. Girod *et al.*, Phys. Rev. Lett **100** 162002 (2008).

[6] S. Stepanyan *et al.*, Phys. Rev. Lett **87** 182002 (2001).

[7] C. Muñoz Camacho *et al.*, Phys. Rev. Lett **97** 262002 (2006).

[8] M. Guidal, M.V. Polyakov, A.V. Radyushkin, M. Vanderhaeghen, Phys. Rev. **D72** 054013 (2005).

[9] N. Kivel, M.V. Polyakov, M. Vanderhaeghen, Phys. Rev. **D63** 114014 (2001).

[10] N. Nekipelov *et al.*, J. Phys. **G34** 627 (2007).

[11] R. De Masi *et al*, Phys. Rev. **C77** 042201 (2008).

[12] S. Morrow *et al*, Eur. Phys. J. **A39** (2009).

[13] S.V. Goloskokov and P. Kroll, Eur. Phys. J. **C42** 281 (2005);
S.V. Goloskokov and P. Kroll, Eur. Phys. J. **C50** 829 (2007).

[14] M. Guidal and S. Morrow, arXiv:hep-ph/07113743 (2007).

[15] J.M. Laget, Phys. Rev. **D70** 054023 (2004);
F. Cano and J.M. Laget, Phys. Lett. **B551** 317 (2003).

[16] C. Hadjidakis *et al.*, Phys. Lett. **B605** 256 (2005).

[17] D.G. Cassel *et al.*, Phys. Rev. **D24** 2787 (1981).

[18] A. Airapetian *et al.*, Eur. Phys. J. **C17** 389 (2000).

[19] M.R. Adams *et al.*, Z. Phys. **C74** 237 (1997).

[20] B. Moreno, PoS Confinement8 079 (2008);
B. Moreno, Thèse de doctorat, Université Paris-Sud 11 (2009).

[21] A. Fradi, `http://indico.cern.ch/contributionDisplay.py?contribId=303&sessionId=4&confId=53294`;
A. Fradi, Thèse de doctorat, Université Paris-Sud 11 (2009).

[22] CLAS12 web site, `http://www.jlab.org/Hall-B/clas12/`;